Ferroelectrics, 1996, Vol. 184, pp. 21–30
Reprints available directly from the publisher
Photocopying permitted by license only

CRYSTAL CHARACTERIZATION BY NONCOLINEAR FREQUENCY DOUBLING

A. REICHERT, K. U. KASEMIR AND K. BETZLER
Fachbereich Physik, Universität Osnabrück, FRG

(Received July 4, 1995; in final form November 27, 1995)

Abstract Noncolinear frequency doubling (NCFD) is discussed as a sensitive technique for the characterization of acentric crystals. Two methods can be applied: 'Spontaneous' NCFD where light scattered at crystal imperfections is used as second fundamental beam and 'induced' NCFD where the usage of a second laser beam yields three-dimensional spatial resolution. Experimental investigations of pure and VTE-treated lithium niobate and of domain boundaries in potassium niobate are presented.

INTRODUCTION

For the application of electrooptic crystals a reliable reproducibility of their relevant physical properties is of great importance. To check composition and homogeneity, which influence these properties, various characterization methods are used. Usually these techniques do not measure the desired parameters directly but other physical properties which depend strongly on composition or doping. Typical methods for the case of e. g. lithium niobate are the measurement of the Curie temperature[1], optical absorption edge[2], refractive indices[3], birefringence[4, 5], or optical second harmonic generation[6, 7]. One of the most sensitive of these methods is the optical second harmonic generation (SHG) which – by measuring phase matching conditions – can detect crystal composition and its spatial variation.

Here we describe two recently developed new SHG methods which utilize the phase matching conditions for second harmonic light generated by two *noncolinear* fundamental beams for crystal characterization.

One of these methods, spontaneous noncolinear frequency doubling (SNCFD), uses scattered light as second fundamental beam; a cone of second harmonic light results. The parameters of the cone reflect the properties of the investigated crystal. Examples of possible experimental setups for a two-dimensional crystal characterization and some results are shown.

Using two slightly focussed beams which intersect each other, second harmonic light generated in the small intersection volume – which is limited in all three spatial dimensions – can be measured. With this method, induced noncolinear frequency doubling (INCFD), it is for the first time possible to visualize the three-dimensional composition profile of a crystal without cutting it. As an example measurements on vapor transport equilibrated (VTE) $LiNbO_3$ are shown. After the inspection of the crystal by INCFD a continuation of the VTE process is possible.

As the SHG intensity depends on the crystal orientation, INCFD also allows a three-dimensional detection of the domain structure in electrooptic crystals. When the interaction volume is moved from one domain to another, the change in the orientation of the SHG tensor leads to a corresponding change in the intensity of the second harmonic light. The detection of 90°-domain walls in $KNbO_3$ is presented as example for the technique.

FUNDAMENTALS OF NONCOLINEAR FREQUENCY DOUBLING

In the case of conventional – colinear – second harmonic generation, phase matching is achieved when the quasi-scalar relation for momentum conservation

$$|\vec{k}_2| = |\vec{k}_1| + |\vec{k}_1'| \tag{1}$$

is fulfilled, where the wave vectors $\vec{k}_1$ and $\vec{k}_1'$ for the fundamental beams and $\vec{k}_2$ for the generated harmonic wave are all parallel to each other.

The phase matching temperature is the parameter which characterizes the crystal composition when noncritical phase matching for second harmonic generation (SHG) is applied. Using a focussed fundamental laser beam permits a two-dimensional investigation of the crystal composition with a high spatial resolution (spatially resolved second harmonic generation, SRSHG)[8]. Similar results can be achieved by using an expanded laser beam and a two-dimensional detector array[9].

In contrast to this, noncolinear frequency doubling (NCFD) utilizes two light beams inclined to each other to fulfill the vectorial phase matching condition

$$\vec{k}_2 = \vec{k}_1 + \vec{k}_1'. \tag{2}$$

The second necessary fundamental beam can be taken from scattered light in the crystal (spontaneous NCFD) or explicitely as second laser beam (induced NCFD). In the latter case a fully three-dimensional topographical resolution is possible due to the interaction volume being limited in all three spatial dimensions.

The angle enclosed by the two fundamental beams, i. e. the angle between $\vec{k}_1$ and $\vec{k}_1'$, can be used as an additional experimental parameter which allows the adjustment of the the phase matching conditions for this nonlinear process in a flexible way.

SPONTANEOUS NON-COLINEAR FREQUENCY DOUBLING

If an intense laser beam hits the crystal surface perpendicularly, most of the light passes inside unrefracted ($\vec{k}_1$). A certain amount of light, however, is scattered by crystal imperfections. If the angle 2φ between the fundamental beam and any of these scattered beams (e.g. $\vec{k}_1'$) fulfills the non-colinear phase matching condition $\sum \vec{k} = 0$, frequency doubled light is generated and amplified ($\vec{k}_2$)[10, 11, 3]. In $LiNbO_3$ both the fundamental beam ($\perp$ c–axis) and the scattered beams may be polarized ordinary. Second harmonic light then is generated at the so called SNCFD-angle φ':

$$\varphi' = \arcsin\left(n_e(2\omega)\sqrt{1 - \frac{n_e^2(2\omega)}{n_o^2(\omega)}}\right) \tag{3}$$

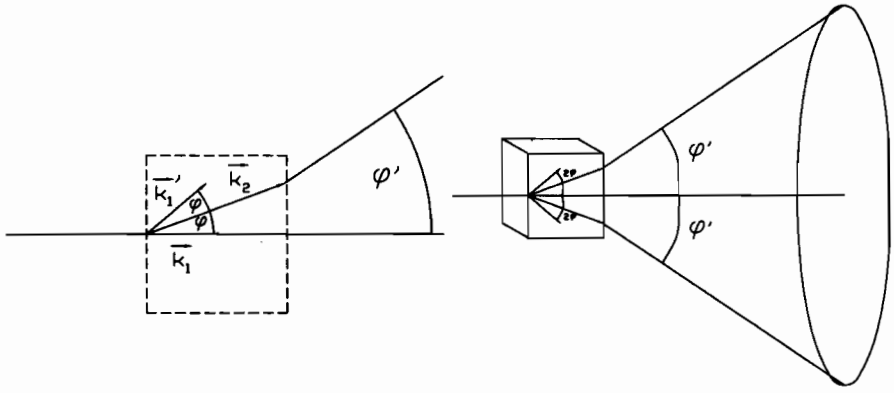

FIGURE 1: SNCFD principle

measured outside the crystal, n_o : ordinary index, n_e : extraordinary index for the respective direction.

The set of phase matching conditions between fundamental and scattered light beams leads in general to an elliptic cone of second harmonic light.

Experimental Setup

For measuring SNCFD we used the setup sketched in fig. 2. A Q-switched Nd:YAG-laser (1064 nm, 1 kHz, ≈10 kW) served as light source. This results in a 532 nm extraordinary second harmonic beam. Two crossed polarizers P and a half-wave plate $\lambda/2$ are used to fine-tune laser intensity and achieve ordinary polarisation of the fundamental beam. After focussing (L_1) the beam onto the crystal C the emanating cone of frequency-doubled light is projected onto a screen (L_2, S) which is scanned by a CCD camera. The BG18 filter blocks the fundamental beam. To

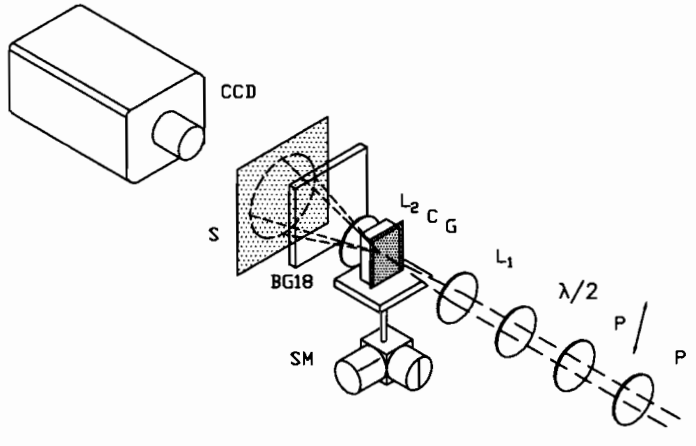

FIGURE 2: Experimental setup for measuring SNCFD.

enhance the amount of scattered light a ground glass plate G can be placed at the crystal surface. By moving the sample with two stepper motors (SM) a two-dimensional spatial resolution is realized.

Detecting Ellipses via Hough Transformation

Projecting the cone of second harmonic light onto the screen yields an elliptical ring. In addition, a central spot (b) due to colinear SHG and some noise appears. As a two-dimensional spatially resolved scan of the crystal results in up to some thousand ring pictures, it is necessary to use an automatic evaluation algorithm for the ring parameters.
An ellipse with one principal axis parallel to the x axis, center at (x_0, y_0), and radii r_x, r_y is defined by:

$$\frac{x - x_0}{r_x}^2 + \frac{y - y_0}{r_y}^2 = 1. \qquad (4)$$

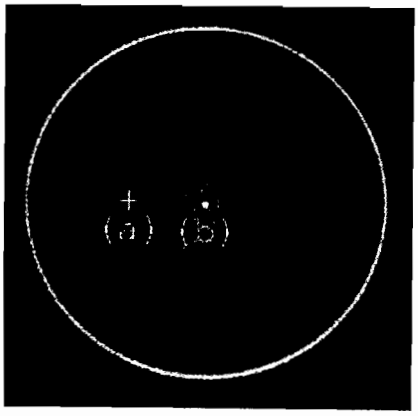

FIGURE 3: SNCFD-Ring.

The first attempt was to use a nonlinear least-square-fit procedure to fit eq. 4 to the measured intensity pattern $I(x, y)$. This method turned out to be very fast but more or less incorrect in the presence of noise even after masking out the center spot.

In contrast to this the Hough method [12], an image processing technique for the detection of shapes that can be described as parametric curves, has the advantage of being relatively unaffected by gaps, noise and shapes different from the one you are looking for. Unlike least-squared-error fitting it does not work in image space but in parameter space defined by the parameters which describe the shape of the curve. In principle the maximum of a probability function in this parameter space has to be found. In our case this probability function in the four-dimensional parameter space of eq. 4 is defined by

$$P(x_0, y_0, r_x, r_y) = \sum_{x,y,\text{eq. 4}} I(x, y) \qquad (5)$$

where I is the pixel intensity and the summation has to be carried out for all (x, y) obeying eq. 4.

The drawback of this 'classical' Hough Transform is the huge parameter array needed which is only sparsely filled because not all r_y/r_x-ratios are possible. So the hits in P do not cumulate well enough to show an expressed maximum.

Better results are achieved applying the Hough transform with a modified parameter space which utilizes the fact that all SNCFD-rings of an investigated

crystal show an r_y/r_x-ratio in a highly restricted range. Consequently we define an 'elliptical circle' based on the transformed parameters $x_0, y_0, r := r_x, e := r_y/r_x$:

$$\sqrt{(x-x_0)^2 + \frac{1}{e^2}(y-y_0)^2} = r. \tag{6}$$

Now in general only small variations in the three-dimensional parameter subspace $\{x_0, y_0, e\}$ have to be involved. The resulting one-dimensional Hough accumulator array $P(r)$ has to be evaluated (smoothing, background subtraction etc.) and varied as a function of the three other parameters until an optimal r is found. The

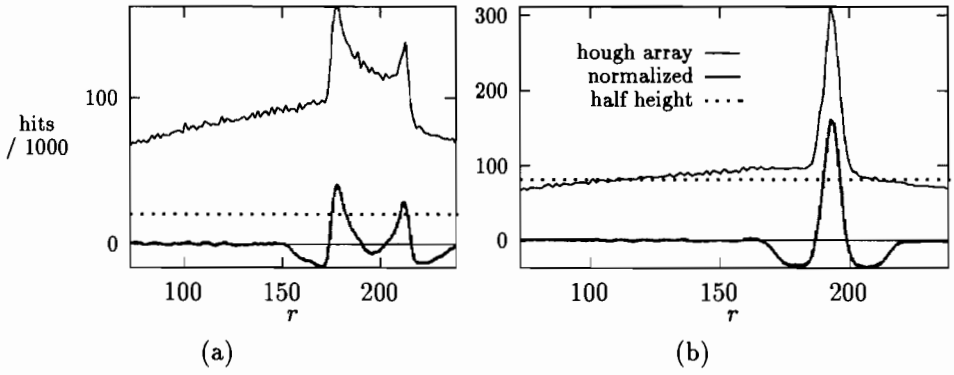

FIGURE 4: Hough accumulator arrays for fig. 3

principle is demonstrated in fig. 4, where in (a) the Hough accumulator array for an intermediate state in the optimization procedure (x_0, y_0 at point **a** of fig. 3) and in (b) that for optimized parameters, is shown (x_0, y_0 at point **b** of fig. 3).

Results

Fig. 5 shows the two-dimensional composition topography of a slice which was cut out of the middle of a VTE treated $LiNbO_3$ crystal (see next chapter for details). While the crystal center shows nearly the initial congruent composition, the Li-content increases to the border due to VTE induced diffusion.

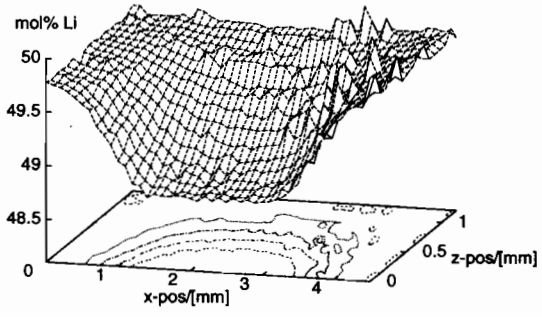

FIGURE 5: Two-dimensional composition topography of a VTE treated $LiNbO_3$ crystal measured by SNCFD.

To show the high resolution provided by SNCFD, a highly homogeneous sample crystal was investigated, $LiNbO_3$ grown from a melt containing a certain amount of potassium [13]. As can be derived from fig. 6, composition changes less than 0.01 % Li_2O can be resolved by the method.

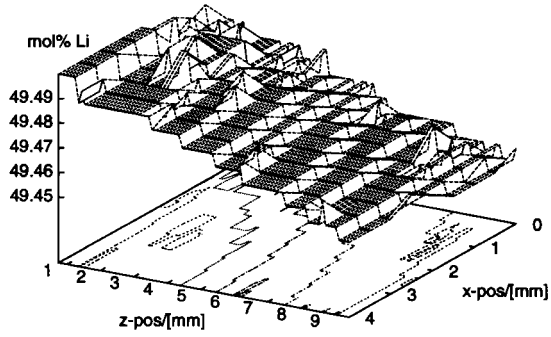

FIGURE 6: SNCFD topography of a highly homogeneous $LiNbO_3$ crystal grown from a potassium-enriched melt.

INDUCED NONCOLINEAR FREQUENCY DOUBLING

In contrast to SNCFD, for INCFD the two fundamental beams are taken in a symmetric way from the laser light, forcing a restricted interaction volume.

Experimental Arrangement

The experimental arrangement for measuring INCFD is sketched schematically in figure 7. The light of a pulsed Nd:YAG–laser is split into two parallel beams of approximately equal intensity. The two beams are then focussed onto the same spot

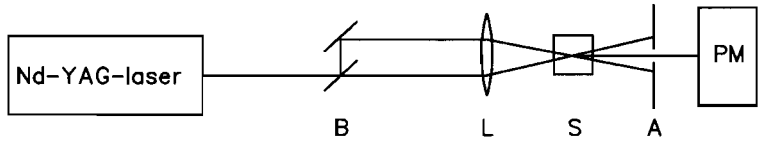

FIGURE 7: Experimental arrangement for measuring INCFD. B: beam splitter, L: focussing lens, S: temperature controlled sample holder, moveable in all three spatial directions, A: aperture for blocking the fundamental beams, PM: photomultiplier.

inside the sample crystal, the interaction angle 2φ is controlled by the distance between the two beams and the focal length of the focussing lens taking into account the refraction at the sample surface. The sample position can be controlled by a three-dimensional linear translation stage with μm resolution. The second harmonic intensity is measured by a photomultiplier with suitable pulse detection electronics as a function of the four parameters position {x, y, z} and sample temperature.

An evaluation with respect to the temperature yields the three-dimensional topography of the (noncolinear) phase-matching temperature which can be referred to a topography of the composition or doping of the material [14].

Results: Monitoring VTE in lithium niobate

One of the most important anorganic electrooptic materials is lithium niobate. Though generally referred to as $LiNbO_3$, it is usually grown at its congruent melting point exhibiting a significant deficit of Li_2O. To fabricate stoichiometric $LiNbO_3$, several techniques have been developed, e. g. growing in potassium-enriched melt [13] or vapor transport equilibration (VTE) [15, 16]. The latter, a post-growth heat treatment in $LiNbO_3$ powder, has the ability to produce every desired composition between the congruent (48.4 % Li_2O) and the stoichiometric one (50 % Li_2O).

As VTE is a diffusion technique, it is of great interest to monitor the generated diffusion profiles in order to control the whole treatment. This monitoring task can be done by INCFD.

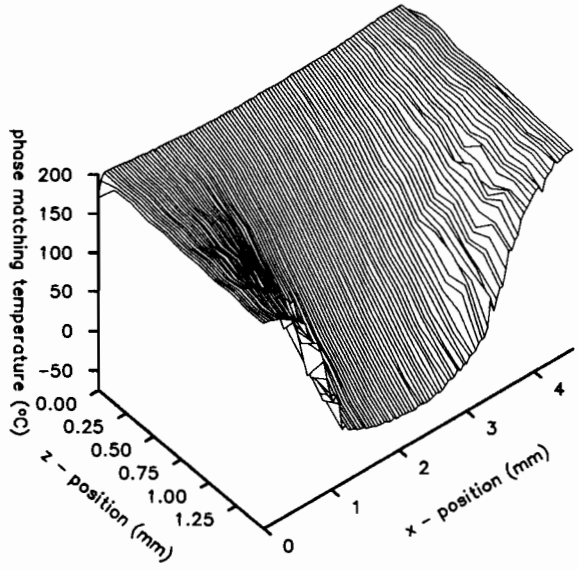

FIGURE 8: Topography of the INCFD phase matching temperature in the central xz-plane of a VTE treated $LiNbO_3$ crystal (for a better overview only about half of this topography from z=0 – the edge of the crystal – upto z=1.5 mm is drawn). The phase matching temperature is a measure for the Li content in the crystal.

For our investigations we fabricated a sample crystal using the VTE technique described by Jundt et al.[16]. We used an approximately $4 \times 4 \times 4$ mm sized $LiNbO_3$ crystal cut from a boule which had been congruently grown by the Czochralsky method. The crystal was treated by VTE for about 200 hours at a temperature of 1100 °C, indiffusion of Li was permitted from each of the six crystal faces. The resulting diffusion topography in two directions (x and z) as measured by INCFD is shown in Fig. 8. As a measure for the Li-content the (noncolinear) phase-matching temperature is plotted as a function of the spatial coordinates x and z in the central xz-plane of the crystal.

To get the diffusion profiles in certain crystallographic directions, these directions can be extracted from the complete picture. This is done in Fig. 9 for the

z-direction. To get an estimate of the spatial resolution of the measurement, the

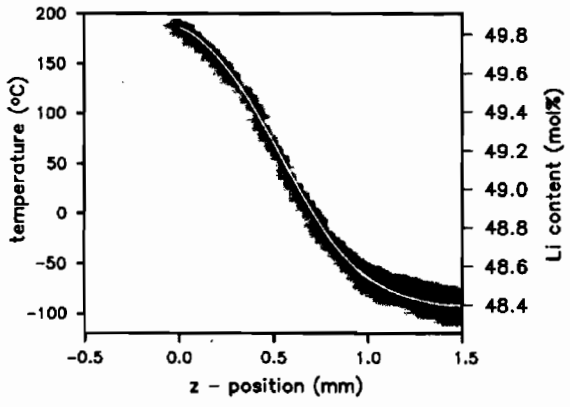

FIGURE 9: SHG-intensity as a function of the temperature and the z-position of a VTE treated $LiNbO_3$ crystal. The white line marks the maximum intensity and thus the phase-matching temperature. The right axis denotes the corresponding Li content.

distribution of the second harmonic intensity is shown as shaded area. Concerning the halfwidth of the second harmonic intensity distribution, the resolution is approximately 30 μm perpendicular to the main beam direction and 200 μm in beam direction. In a simple diffusion geometry like in the VTE example the detection of the intensity maximum — thus the effective resolution — can of course be done with better accuracy.

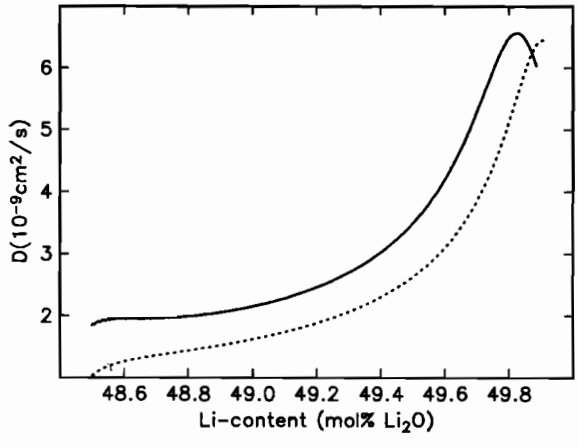

FIGURE 10: Composition dependence of the diffusion constants for Li in lithium niobate at 1100 °C parallel (full line) and perpendicular (dashed line) to the polar axis (z-direction) of the crystal.

From the profile measurements the diffusion constants for Li in lithium niobate can be derived[17]. For our treatment temperature of about 1100 °C we find that the diffusion constants parallel and perpendicular to the z-direction (polar axis) are slightly different and vary as a function of the composition[18]:

$$D_{\parallel} = 1.8\ldots6.5\times10^{-9}\ \mathrm{cm^2/s} \quad \text{for} \quad c_{Li} = 48.5\ldots49.8\ \%$$
$$D_{\perp} = 1.0\ldots6.5\times10^{-9}\ \mathrm{cm^2/s} \quad \text{for} \quad c_{Li} = 48.5\ldots49.8\ \%.$$

The exact composition dependence of the two principal diffusion constants is depicted in Fig. 10.

Results: Domain walls in potassium niobate

INCFD – just as second harmonic generation in general – depends strongly on the orientation of the investigated crystal. As both the nonlinear susceptibility and the refractive indices change abruptly when the geometrical orientation of the crystal changes, INCFD can be used for a topographical detection of domain boundaries inside a crystal. Domain boundaries will show up as intensity steps in the three-dimensional INCFD intensity field. These intensity steps can be automatically evaluated using numerical differentiation and involving the maxima of the derivative field.

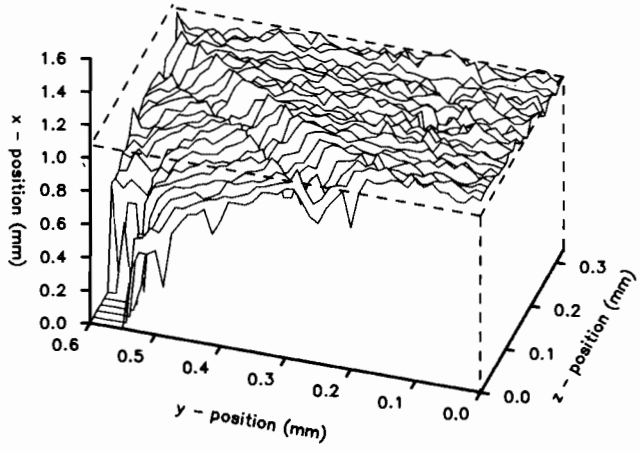

FIGURE 11: INCFD measurement on a $KNbO_3$ crystal for detecting the boundary between two ferroelectric domains. The outline of the investigated crystal is indicated by dashed lines. The full lines connect the maxima of the three-dimensional derivative field which was generated by a numerical differentiation of the INCFD intensity field.

An example is given in Fig. 11. INCFD was measured on a potassium niobate crystal with two domains oriented 90° to each other. The overall size of the investigated part of the crystal was about $0.3 \times 0.6 \times 1.1$ mm. The measurement was done at constant temperature using highly focussed beams (working with highly focussed beams and thus enlarged beam divergence $\Delta\varphi$ is no drawback in this type of measurements as only a high spatial resolution in the detection of the domain boundaries is of importance). The angle between the interacting fundamental beams was chosen such that phase matching was achieved in the larger of the two domains ($\varphi' = 8.8°$, T= 190 °C, usage of the tensor element d_{32}). Doing this, optimal contrast and – in combination with the strong focussing – a spatial resolution of approximately 10 μm could be achieved.

In Fig. 11 the maxima of the derivative field are connected by full lines. At the right these lines indicate the border plane of the crystal, at the left the border between the two 90° domains in the crystal.

CONCLUSION

Noncolinear frequency doubling offers, with the two techniques SNCFD and INCFD, very sensitive methods for the characterization of acentric – especially electrooptic – crystals. Both techniques enable an accurate two- or three-dimensional topographical inspection of the crystal composition; for the example of lithium niobate the resolution is much better than 0.01 mol% Li_2O. Furthermore, it is possible to locate imperfections in crystals by INCFD, as e. g. domain boundaries.

ACKNOWLEDGEMENTS

We are greatly indebted to Prof. S. Kapphan and Prof. O. Schirmer for providing the $LiNbO_3$ crystals, Dr. H. Hesse for the $KNbO_3$ crystal, and G. Steinhoff for a careful treatment and preparation of the samples. Financial support from the Deutsche Forschungsgemeinschaft (SFB 225, A 10) is gratefully acknowledged.

REFERENCES

1. J. R. Carruthers, G. E. Peterson, M. Grasso, and P. M. Bridenbaugh, J. Appl. Phys. **42**, 1846 (1971).
2. I. Földváry, K. Polgár, R. Voszka, and R. N. Balasanyan, Crystal Res. & Technol. **19**, 1659 (1984).
3. U. Schlarb and K. Betzler, Phys. Rev. **B50**, 751 (1994).
4. J. G. Bergman *et al.*, Appl. Phys. Lett. **12**, 92 (1968).
5. E. Born, E. Willibald, and R. Veith, Proc. IEEE Ultrasonics Symp. 268 (1984).
6. H. Fay, W. J. Alford, and H. M. Dess, Appl. Phys. Letters **12**, 89 (1968).
7. N. Schmidt, K. Betzler, and B. C. Grabmaier, Appl. Phys. Lett. **58**, 34 (1991).
8. N. Schmidt, K. Betzler, and S. Kapphan, Cryst. Latt. Def. and Amorph. Mat. **15**, 103 (1987).
9. N. Schmidt *et al.*, J. Appl. Physics **65**, 1523 (1989).
10. J.A.Giordmaine, Phys. Rev. Letters 8, 19 (1962).
11. U. Schlarb and K. Betzler, Phys. Rev. **B48**, 15613 (1993).
12. D.H. Ballard and Chr.M. Brown, *Computer Vision* (Prentice-Hall, 1982), p. 119ff.
13. G. I. Malovichko *et al.*, Appl. Phys. A **56**, 103 (1993).
14. U. Schlarb and K. Betzler, Ferroelectrics **156**, 99 (1994).
15. Y. S. Luh, M. M. Fejer, R. L. Byer, and R. S. Feigelson, J. Cryst. Growth **85**, 264 (1987).
16. D. H. Jundt, M. M. Feijer, and R. L. Byer, IEEE J. Quantum Electron. **26**, 135 (1990).
17. D. H. Jundt and M. M. Fejer, J. Appl. Phys. **72(8)**, 3468 (1992).
18. A. Reichert and K. Betzler, (unpublished).